chem2Dmat

AUGUST 31 - SEPTEMBER 03, 2021 • ONLINE

FZU Fyzikální ústav Akademie věd České republiky
Institute of Physics of the Czech Academy of Sciences

3D-Graphene based Pressure and Strain Sensor

Prabhat Kumar*, Martin Šilhavík, Zahid Ali Zafar, and Jiří Červenka

Department of Thin Films and Nanostructures, Institute of Physics of the Czech Academy of Sciences, Prague 16200, Czech Republic

kumarp@fzu.cz

NMS FZU

Abstract

We demonstrate a broad range and fast response pressure and strain sensor using a flexible and conductive 3D graphene structure. The sensor can detect small pressures/strains and various biological signals from the movement of human skin. The active element of sensor consists of a 3D graphene nanoporous framework made of graphene sheets separated with air-filled pores. A simple hydrothermal technique followed by freeze-drying and high-temperature thermal annealing is used for the synthesis of 3D graphene aerogel. The resulting graphene aerogel is highly elastic and the contact resistance between aerogel and rigid metal electrode is highly sensitive to applied stimuli. The extraordinary sensitivity of the contact resistance permits the detection down to a few micrometers by a small change of the sample size. In addition, the elastic nature of graphene aerogel provides high responsivity to the sensor, allowing detecting fast actions down to a few milliseconds and temperature independent. We show that the 3D graphene-based sensors can be used as wearable electronic sensors for diverse kinds of biological motion detection, human-machine interface and soft robotics applications.

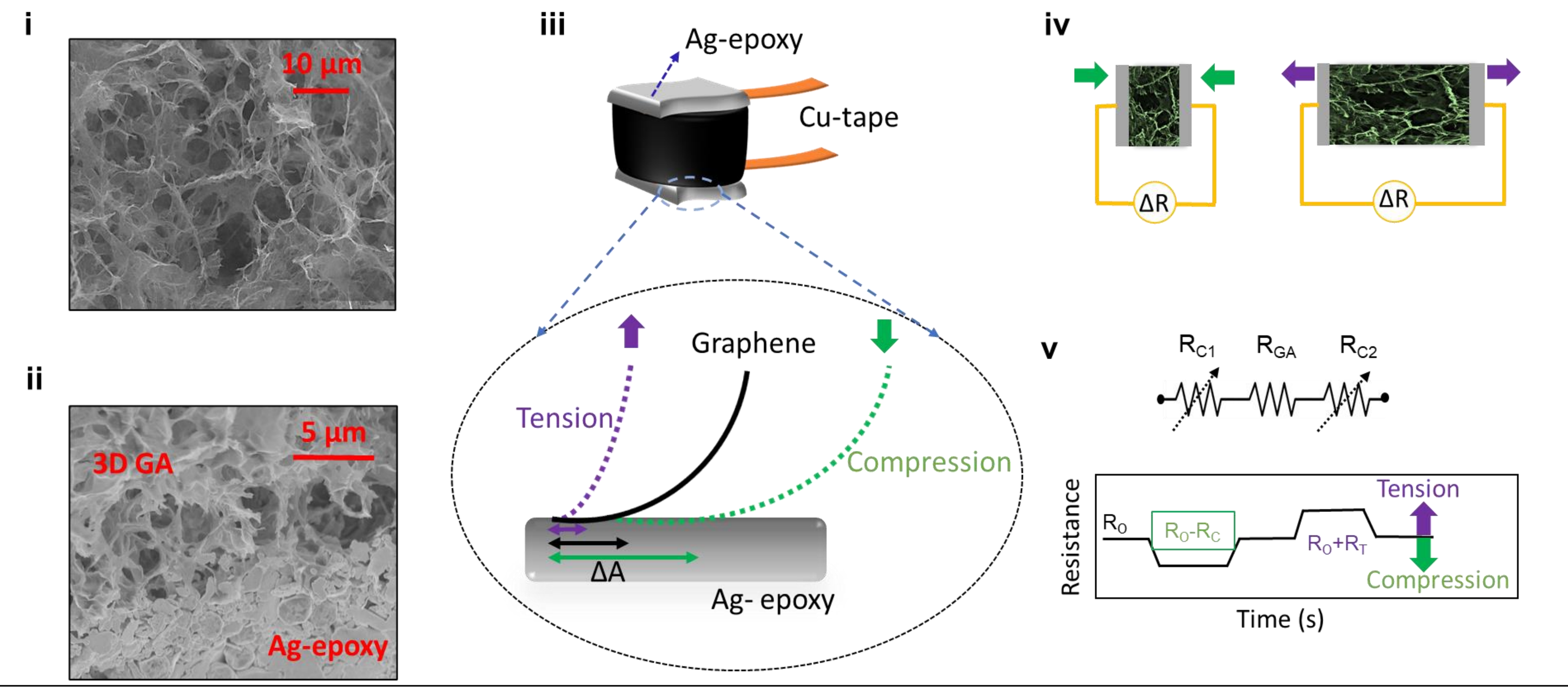

Objectives

- For human-machine interface and skin monitoring devices, the pliable nature of the skin requires sensors with a wide dynamic range and high sensitivity 0.2-500 kPa.
- There is no electromechanical sensor that would cover such a high range in tensile and compression.
- The traditional piezoresistive sensors based on bulk piezo resistivity variation have a limited range of operation, and are not suitable for measuring different physiological signals.
- The development of novel sensing mechanisms and materials that can emulate strain and pressure-sensing properties of natural skin.

Experimental

Synthesis of 3D graphene

Figure 1: Actual pictures of the materials obtained after every step of synthesizing 3D graphene aerogels (scale bar: 1 cm).

Characterization of Graphene Aerogels

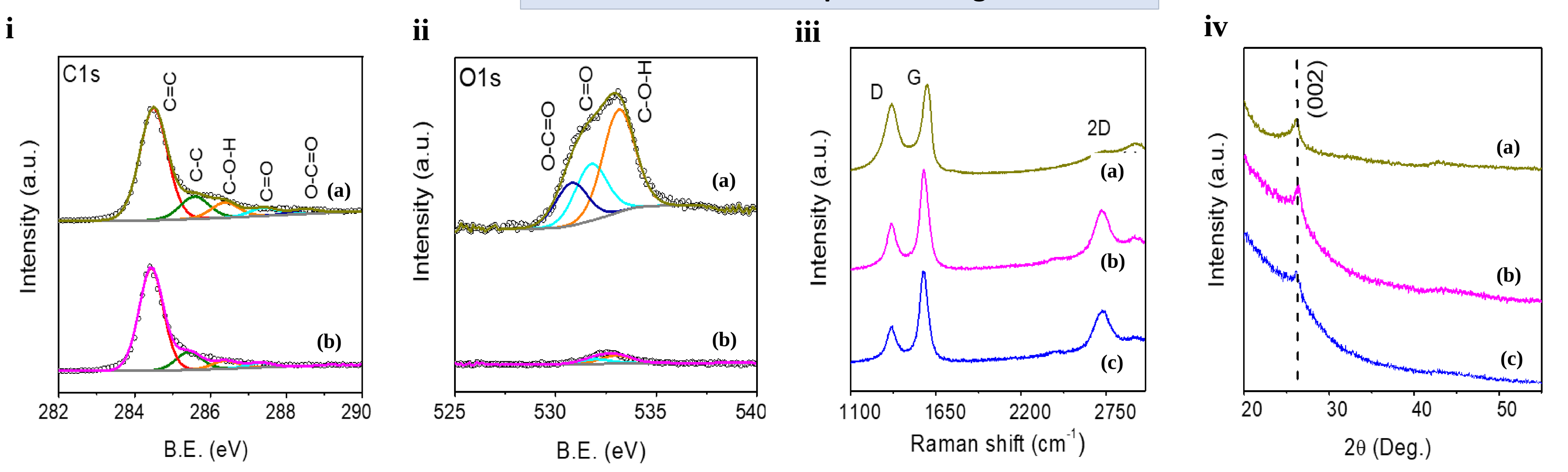

Figure 2: (i-ii) XPS spectra of C 1s and O 1s of graphene aerogel (a) before and (b) after annealing. (iii) Raman spectra and (iv) X-ray diffractograms of the graphene aerogel (a) before annealing (dark yellow) (b) after annealing (magenta) and (c) 70% compressed sample (blue).

Results and Discussion

Sensor Characterization

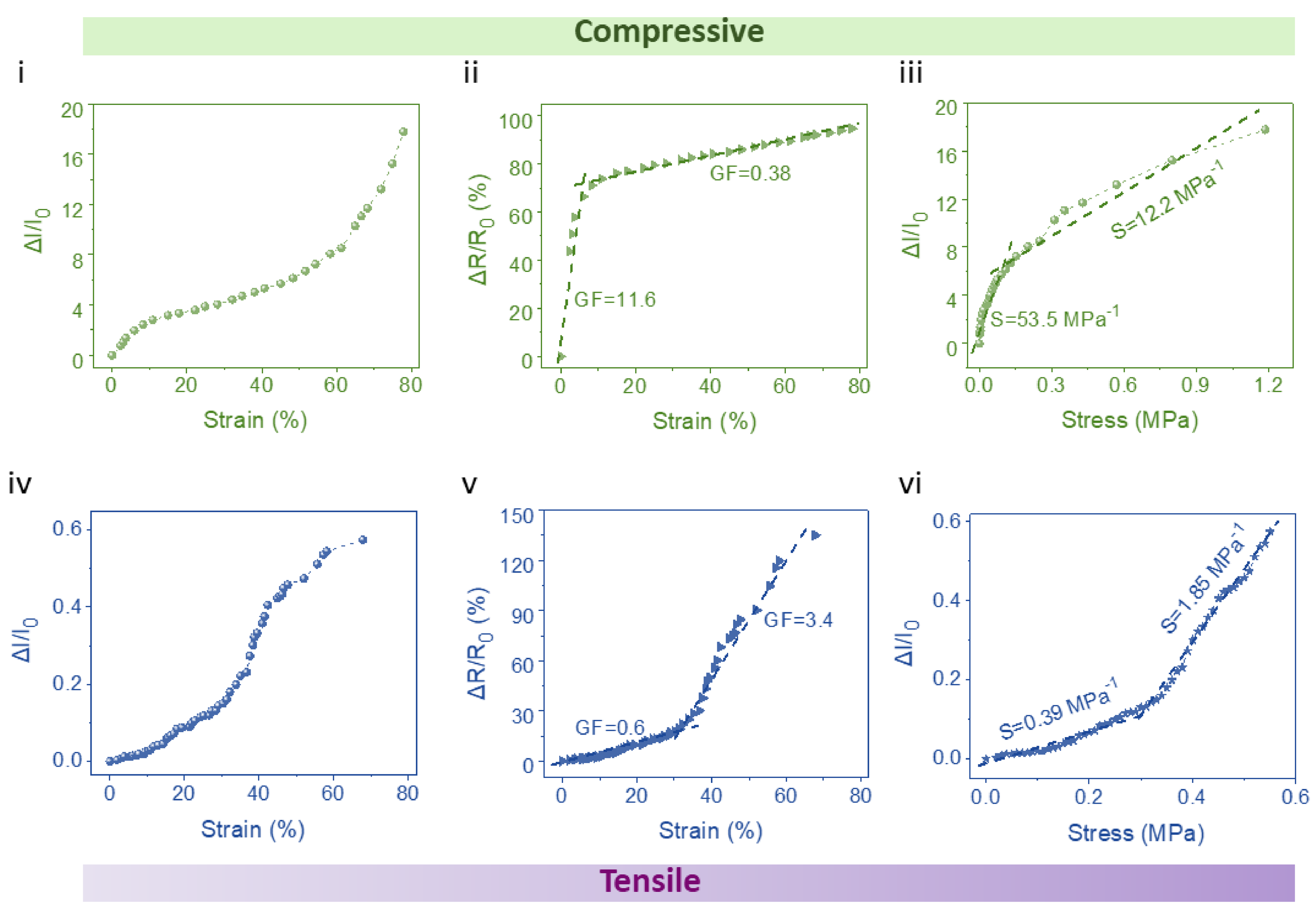

Figure 3: Electrical response of GA strain sensors under compression and tension. (i and iv) Current ($\Delta I/I_0$) response and (ii and v) relative resistance change ($\Delta R/R_0$) of GA sensors with applied compressive and tensile stress, respectively. (iii and vi) The current response of the GA sensors as a function of compressive and tensile stress, showing two sensitivity regimes. The slope of the curves was used to calculate the gauge factor (GF = $(\Delta R/R_0)/\varepsilon N$) and sensitivity (S = $(\Delta I/I_0)/\Delta P$) of the sensors.

Sensing mechanism

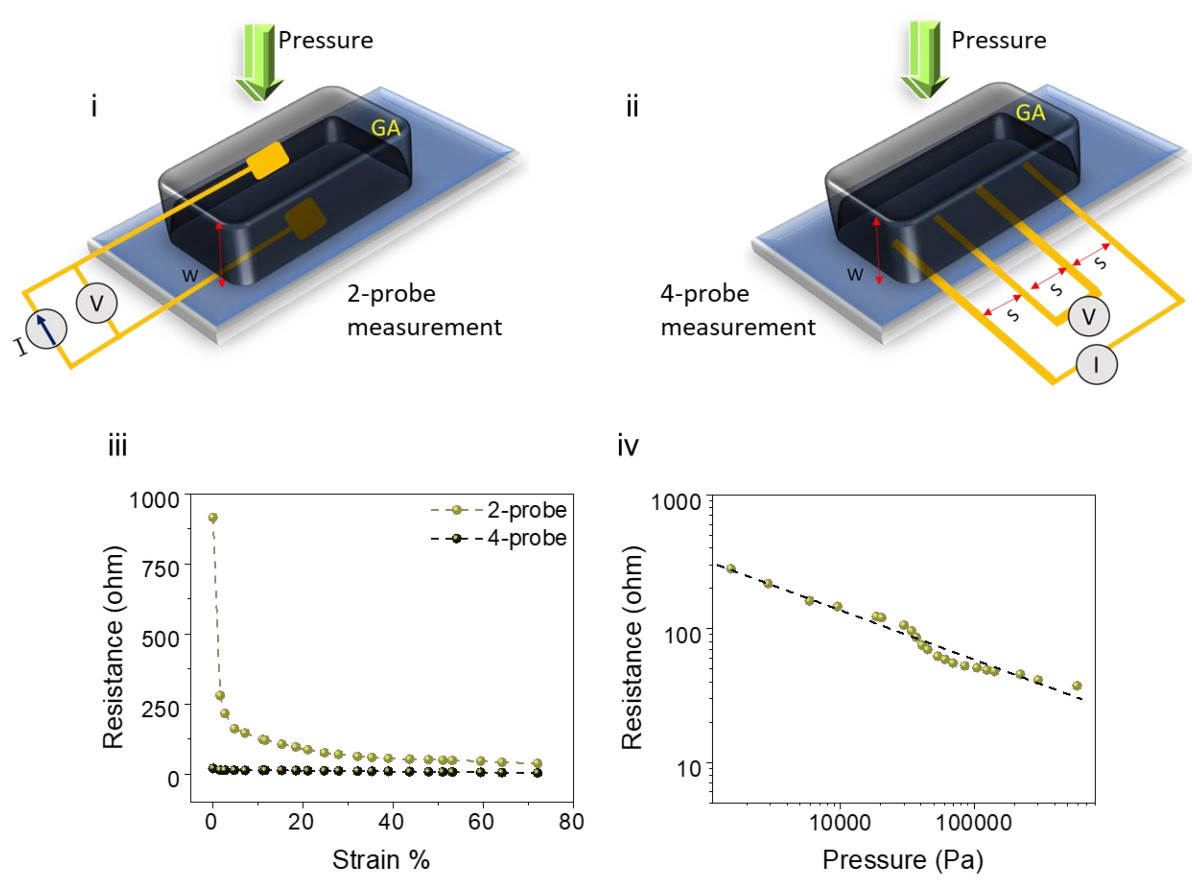

Figure 4: (i-ii) Schematics of experimental set-ups for contact resistance measurements in two-probe and four-probe configurations. (iii) Measured resistance of the device under stress using the 2-probe and 4-probe methods. (iv) Relationship between resistance and pressure in a log(R) and log(P) scale using the 2-probe method.

Dynamic Response and Sensor Performance

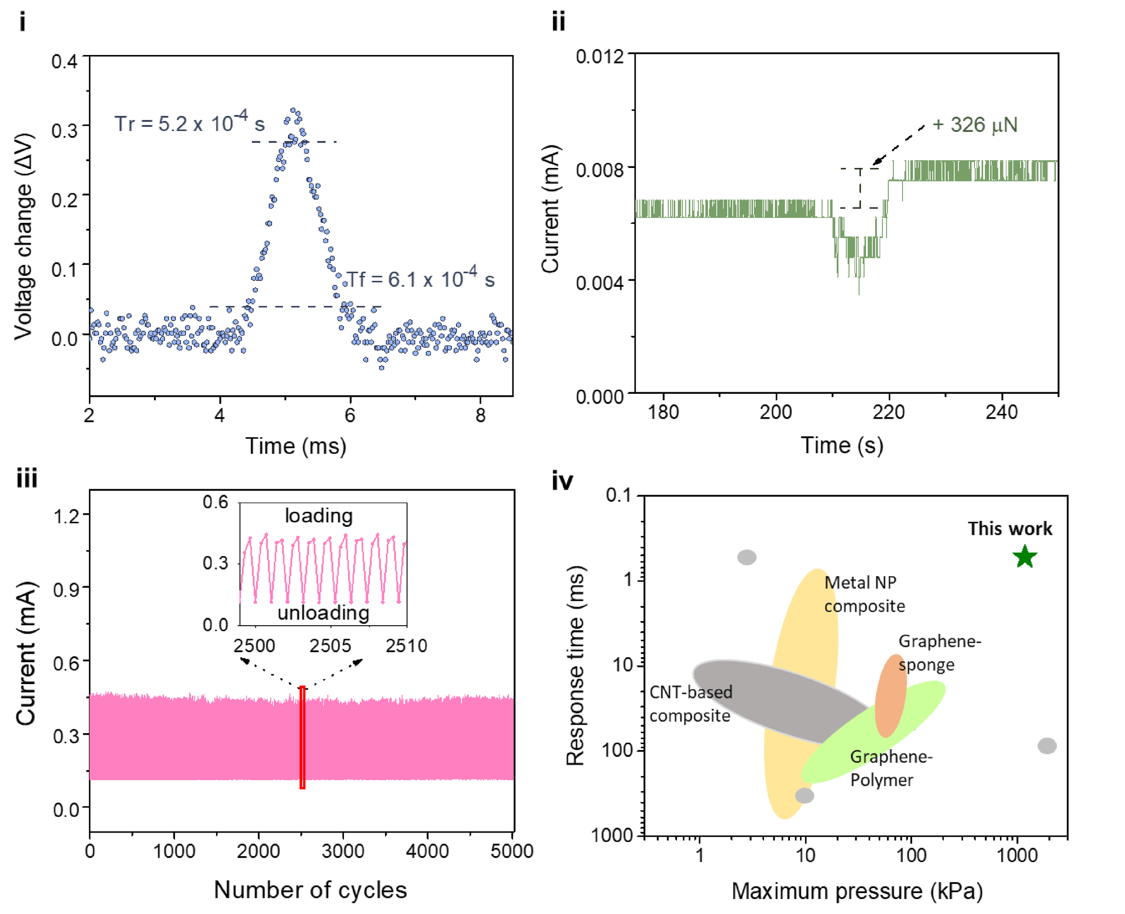

Figure 5: (i) The instant voltage response of a GA sensor demonstrating the response time of 0.52 ms. (ii) An example of a GA sensor detecting ultralow force (iii) the reproducibility of the pressure sensor after 5,000 loading-unloading cycles. (iv) Comparison of the response time and maximum pressure limit of the GA sensors with different strain sensors based on GA and other materials.

Applications

Human Pulse measurement | Tactile sensing: Weight measurement | Finger movement measurement

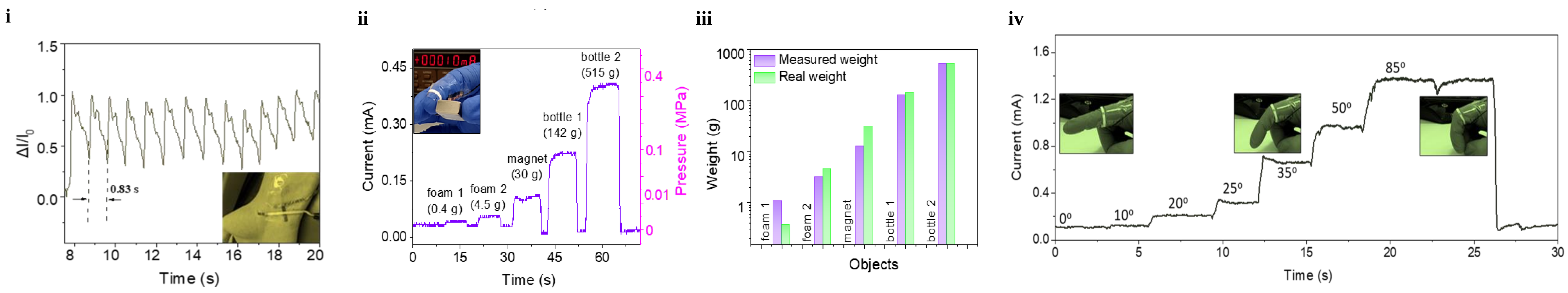

Figure 6: Tactile sensing using a 3D GA sensor. (i) The current ($\Delta I/I_0$) response of a GA sensor attached above the artery of the wrist detecting a pulse as a function of time. (ii) The current response of a GA sensor attached to an index finger when grasping objects of variable weight. The inset shows an optical image of a magnet lifting using the thumb and index fingers. (iii) The real weight and measured weight of different picked objects by the sensor. (iv) The current signals corresponding to finger-bending motions. The inset shows optical images of finger bending with the attached sensor.

Conclusion

- The sensors have demonstrated a remarkably broad working range both in tensile (0-0.55 MPa) and compressive (0-1.18 MPa) stress, which enables them to cover the whole range of human bodily actions.
- The sensors have also shown high sensitivity with a gauge factor in the range of 0.38-11.6 in the compressive mode and 0.6-3.4 in the tensile mode, respectively.
- The sensors provide long-term stability over 5000 compressing–relaxing cycles and a fast response time of 5.2×10^{-4} s. .
- We have proposed that the observed piezoresistive sensing mechanism is originating from the variation of the contact resistance of the interface between the porous graphene aerogel and metal contacts.
- The reported graphene aerogel sensors have a high potential for applications in biomedicine, wearable electronics, and tactile robotic applications.

CONTACT PERSON

Prabhat Kumar*
Department of Thin Films and Nanostructures, Institute of Physics of the Czech Academy of Sciences,
Prague 16200, Czech Republic
kumarp@fzu.cz

REFERENCES

1. Y. Xu, K. Sheng, C. Li and G. Shi, ACS Nano, 2010, 4, 4324–4330.
2. M. A. Worsley, T. T. Pham, A. Yan, S. J. Shin, J. R. I. Lee, M. Bagge-Hansen, W. Mickelson and A. Zettl, ACS Nano, 2014, 8, 11013–11022.
3. S. Luo, Y. A. Samad, V. Chan and K. Liao, *Matter*, 2019, **1**, 1148–12021.
4. M.-H. Bao, in Handbook of Sensors and Actuators, 2000, pp. 199–239.
5. C. Xiang, N. Behabtu, Y. Liu, H. G. Chae, C. C. Young, B. Genorio, D. E. Tsentalovich, C. Zhang, D. V. Kosynkin, J. R. Lomeda, C. C. Hwang, S. Kumar, M. Pasquali and J. M. Tour, ACS Nano, 2013, 7, 1628–1637.
6. J. A. Greenwood and J. B. P. Williamson, Proc. R. Soc. London. Ser. A. Math. Phys. Sci., 1966, 295, 300–319.
7. R. S. Timsit, IEEE Trans. Components Packag. Technol., 1999, 22, 85–98.

Acknowledgments

We acknowledge funding support from the Czech Science Foundation (GACR – Grant No. 19-23986S) and the Operational Programme Research, Development and Education financed by European Structural and Investment Funds and the Czech Ministry of Education, Youth and Sports (SOLID21 - Project No. CZ.02.1.01/0.0/0.0/16_019/0000760).

FYZIKA PEVNÝCH LÁTEK PRO 21. STOLETÍ (SOLID21)
GAČR
EVROPSKÁ UNIE Evropské strukturální a investiční fondy Operační program Výzkum, vývoj a vzdělávání